

# Investigation into the rotational dynamics of the defunct satellite TOPEX/Poseidon

Luc Sagnières<sup>1,2\*</sup>, Inna Sharf<sup>1</sup> and Florent Deleflie<sup>2</sup>

<sup>1</sup>Department of Mechanical Engineering, McGill University <sup>2</sup>IMCCE, Observatoire de Paris

## 1 Introduction

The satellite TOPEX/Poseidon was launched in 1992 and operated successfully until it malfunctioned in January 2006. Since then, it has become one of the largest pieces of space debris in orbit. Defunct spacecraft represent a significant risk to active and future space missions. Active Debris Removal (ADR) has been proposed as a solution to this problem, where a removal spacecraft would be launched, rendezvous with a target, stabilize and capture it, and finally remove it from orbit. However, precise knowledge of the target's rotational parameters ahead of time is key for the stabilization and capture of the debris.

Satellite Laser Ranging (SLR) observations of TOPEX/Poseidon have found that since its end-of-mission, the satellite has been experiencing a consistent increase of its angular velocity. In order to investigate the long-term evolution of its rotational motion in more detail, a novel comprehensive coupled orbit-attitude propagation model, called D-SPOSE, will be used [1]. First, an analytical method to estimate the unknown inertia properties of the spacecraft from SLR observations will be derived. Second, the propagation model will be employed and the influence of external torques, namely the gravity-gradient, solar radiation, and eddy-current torques, will be analyzed, obtaining a better characterization of the evolution of the satellite's rotational motion. Simulation results will then be compared to SLR observations and the effect of internal energy dissipation will be identified.

## 2 Determining Inertia Properties from Observations

A methodology is presented here to produce an estimate of a non-dimensional parameter related to the moments of inertia of the spacecraft. The equation for the rotational motion of a rigid body under external perturbations can be written as a function of its angular momentum,  $\mathbf{h} = \mathbf{I}\boldsymbol{\omega}$ , in the following way:

$$\frac{d\mathbf{h}(t)}{dt} + \boldsymbol{\omega}(t) \times \mathbf{h}(t) = \boldsymbol{\tau}(t, \mathbf{r}(t), \mathbf{v}(t), \mathbf{q}(t), \boldsymbol{\omega}(t)) \quad (1)$$

However, Eq. (1) can also be interpreted as the equation of motion of angular momentum expressed as components in the Earth-Centered Orbital (ECO) frame, defined to be fixed with the precessing orbit as seen in Fig. 1, with  $\mathbf{h} = [h_x \ h_y \ h_z]^T$ , when perturbed by an oblate primary [2]. In this interpretation,  $\boldsymbol{\tau}$  is the sum of the external torques expressed in the ECO frame and  $\boldsymbol{\omega}$

---

\*corresponding author: [luc.sagnieres@mail.mcgill.ca](mailto:luc.sagnieres@mail.mcgill.ca)

represents the angular velocity of the orbital plane, which is a function of the rate of change of the right ascension of the ascending node,  $\dot{\Omega}$ , and the inclination of the orbit,  $i$ .

For a stable principal axis spin, under the sole influence of the conservative gravity-gradient torque, and a circular orbit, it is possible to arrive at the following equation of rotational motion [1, 2]:

$$\begin{bmatrix} \dot{\theta} \cos \theta \cos \lambda - \dot{\lambda} \sin \theta \sin \lambda \\ \dot{\theta} \cos \theta \sin \lambda + \dot{\lambda} \sin \theta \cos \lambda \\ -\dot{\theta} \sin \theta \end{bmatrix} = \frac{3\mu}{4r^3} \frac{H}{h} \cos \theta \begin{bmatrix} -\sin \theta \sin \lambda \\ \sin \theta \cos \lambda \\ 0 \end{bmatrix} - \begin{bmatrix} -\dot{\Omega} \sin \theta \sin \lambda \cos i + \dot{\Omega} \cos \theta \sin i \\ \dot{\Omega} \sin \theta \cos \lambda \cos i \\ -\dot{\Omega} \sin \theta \cos \lambda \sin i \end{bmatrix} \quad (2)$$

where  $H = I_x + I_y - 2I_z$  for a principal axis spin, and  $h = I_z \omega$  assuming it is the principal  $z$ -axis (as was determined from the SLR campaign, see Fig. 3), and with  $\theta$  and  $\lambda$  defined in Fig. 1b, parametrizing the orientation of  $\mathbf{h}$ .

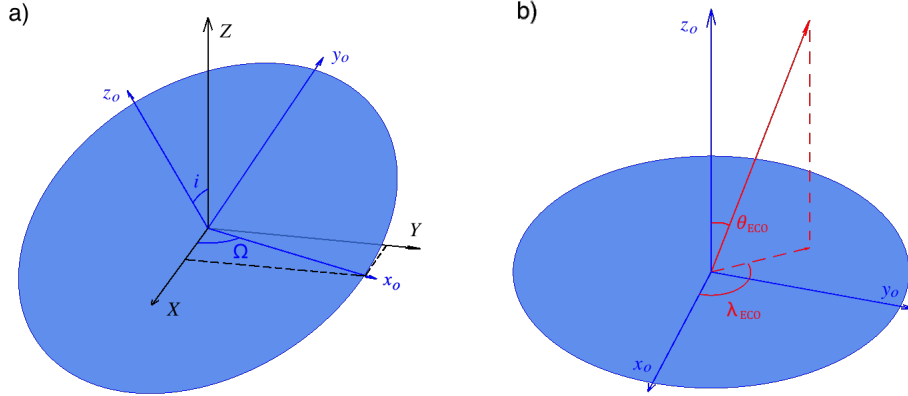


Figure 1: Earth-Centered Orbital Frame

This is a system of three equations that defines the motion of the spin axis in the ECO frame through the angles  $\theta$  and  $\lambda$ , if all other parameters are known. Alternatively, these equations can also be used to identify the value of parameter  $H/h$  if observations of the motion of the spin axis are available, as is the case for TOPEX/Poseidon. Figure 2 displays observations of its spin axis orientation and period as determined by SLR for the time frame from 2014-2017 in the ECO frame [3]. From these observations, it is possible to determine approximate values for  $\theta$ ,  $\lambda$ ,  $\dot{\theta}$ ,  $\dot{\lambda}$ , and  $\omega$  at a specific point in time. Equation (2) can then be solved for the ratio  $H/h$ , which in turn can be written as a function of a non-dimensional parameter  $I^*$ , the latter a function of the moments of inertia:

$$\frac{H}{h} = \frac{I^*}{\omega} \quad (3)$$

$$I^* = \frac{I_x + I_y - 2I_z}{I_z} \quad (4)$$

The most simple observations that can be used from Fig. 2 in order to obtain an estimate of  $I^*$  occur at times when  $\dot{\lambda} = 0$  using the second scalar equation of Eq. (2). Substituting for  $\dot{\theta}$  from the

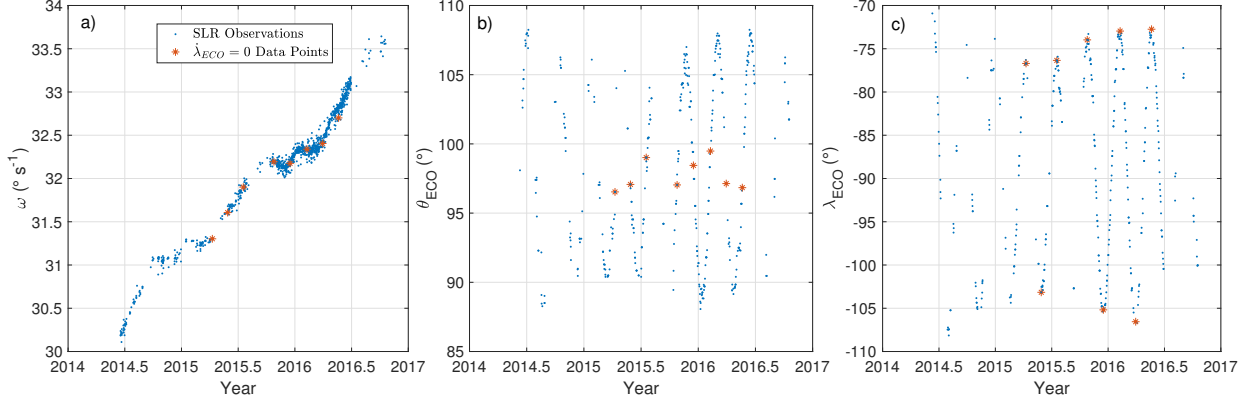


Figure 2: Observations of TOPEX/Poseidon Angular Velocity and Spin Axis Orientation in the ECO Frame

third scalar equation of Eq. (2),  $\dot{\lambda} = 0$ , and solving for  $I^*$ , yields:

$$I^* = \frac{4r^3\omega}{3\mu} \left( -\dot{\Omega} \sin i \csc \theta \sin \lambda + \dot{\Omega} \cos i \sec \theta \right) \quad (5)$$

This simplification is valid as long as  $\theta$  is not a multiple of  $\pi/2$ .

From Fig. 2c, it is possible to select 8 points which satisfy the  $\dot{\lambda} = 0$  condition. The corresponding values of  $\omega$ ,  $\theta$ , and  $\lambda$  are shown by red stars in Fig. 2 and the values of  $r$ ,  $i$ , and  $\dot{\Omega}$  were determined from TLEs at the respective times. The mean and standard deviation of  $I^*$  calculated from the set of 8 points was found to be  $I^* = 0.79 \pm 0.15$ , reflecting a significant spread in these estimates.

As the spacecraft was shown to be rotating about its body-frame  $z$ -axis, this estimate of  $I^*$ , combined with Eq. (5), seems to indicate that the spacecraft can not be rotating about its *major* principal axis. This will now be scrutinized in detail using D-SPOSE.

### 3 Investigation using D-SPOSE

#### 3.1 Simulation Inputs

The initial orbital elements used for the coupled orbit-attitude propagations were taken from a TLE at the time of the first SLR observations shown in Fig. 2:

```
1 22076U 92052A 14163.17066206 -.00000054 00000-0 28497-4 0 2018
2 22076 66.0407 248.1072 0007707 272.4947 118.5262 12.80986122 21470
```

At approximately that epoch, on June 11, 2014, the spin period of TOPEX/Poseidon was determined to be approximately 11.92 s, with  $\theta = 98.10^\circ$  and  $\lambda = -70.92^\circ$  (see Fig. 2).

The spacecraft surface geometry model used, made up of 16 triangular surfaces, is shown in Fig. 3 with the solar panel orientation identified by the red arrow. The spacecraft mass is taken as 2405.4 kg; the center of mass is assumed to be  $\mathbf{c}_p = [0.160 \quad -0.418 \quad 0.049]^T$  m from the center of the box with surface areas  $\Delta x \Delta y = 8.32 \text{ m}^2$ ,  $\Delta x \Delta z = 8.18 \text{ m}^2$ , and  $\Delta y \Delta z = 4.71 \text{ m}^2$ ; the solar array measures 3.3 m in width and has a surface area of  $25.5 \text{ m}^2$  [4]. All of these parameters, as well as the surface optical coefficients, are taken directly from the International DORIS Service (IDS) macro-model for TOPEX/Poseidon [4]. The mass and center of mass are calculated from pre-launch

estimates with the effect from manoeuvres removed [4]. Furthermore, the exact orientation of the solar panel is unknown as during the mission it rotated about the axis going through the center of the solar panel and satellite body and aligned with the body-frame  $y$ -axis; the orientation shown in Fig. 3a is considered to be the  $0^\circ$  case, where rotating it from its current  $-z$  orientation towards the  $x$ -axis is considered positive.

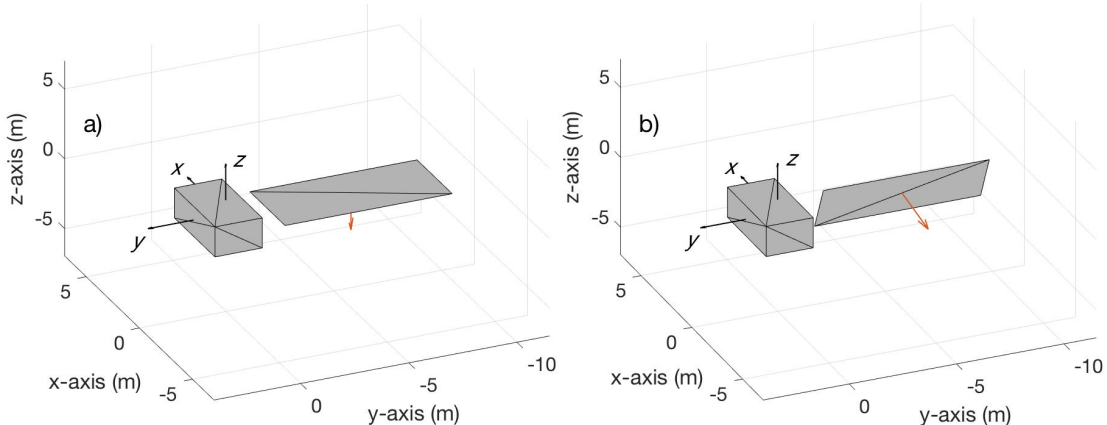


Figure 3: TOPEX/Poseidon Surface Geometry Model with Solar Panel Orientation at: a)  $0^\circ$  and b)  $285^\circ$

Simulations were carried out for a period of three years (1096 days) with a time step of 0.5 s, which was determined to be sufficiently small after doing a work-energy balance check and obtaining almost exactly the same results with a time step of 0.1 s. The gravity-gradient torque and gravitational acceleration were calculated using a geopotential up to order and degree 2. Aerodynamic drag and torque were neglected due to the altitude of the spacecraft (1,340 km). The accelerations and torques due to direct solar radiation, as well as reflected (albedo) and emitted (infrared) radiation were considered, as well as the eddy-current torque using IGRF-12.

As several parameter values of the spacecraft are uncertain, multiple simulations were executed by varying four types of parameters. First, the true moments of inertia are unknown: only a relationship between them was found. Second, although previously estimated to be rotated approximately  $285^\circ$  from the orientation in Fig. 3a, as determined in the study undertaken by the SLR campaign, the exact orientation of the solar panel is unknown [3]. Simulations were therefore performed varying this value from  $275^\circ$  to  $295^\circ$  in  $1^\circ$  increments (the  $285^\circ$  case is shown in Fig. 3b). Third, the effect of the eddy-current torque, which was not included in the attitude dynamics model of the SLR study used to propagate the spin period and obtain the estimate of  $I_z = 70,000 \text{ kg m}^2$ , will be investigated here and the value of the magnetic tensor will be estimated. Finally, the finding that the spacecraft is not spinning about its major axis needs to be confirmed by analyzing the effect of internal energy dissipation as will be done in Section 4.

### 3.2 Propagation Results

Varying all of the parameters outlined above, multiple simulations showed an agreement between propagation results and observations. When including radiation pressure, a slight shift in the oscillations of the spin axis orientation was found to occur with respect to observations. The best fit between simulations and observations for the evolution of the spin axis orientation was found

to occur when  $I^* = 0.83$ , well within the standard deviation of the original mean ( $0.79 \pm 0.15$ ). Therefore, the relationship between the moments of inertia must be:

$$I_x + I_y = 2.83I_z \quad (6)$$

An agreement between simulations and observations for the evolution of the spin period was found for the four cases presented in Table 1. The associated simulations are shown in Fig. 4. The results of the simulations were independent of  $I_x$  and  $I_y$  as long as the relationship in Eq. (6) was held, and for  $I_z < I_x$  and  $I_z < I_y$ . If either  $I_y$  or  $I_x$  was set to a value smaller than  $I_z$ , then a large instability occurred, showing that an intermediate principal axis spin is not plausible. These simulations have so far neglected possible energy dissipation of the spacecraft; this effect needs to be investigated, especially for a spacecraft which seems to be spinning about its minor principal axis.

| Simulation | $I_z$ (kg m <sup>2</sup> ) | $M$ (S m <sup>4</sup> ) | $\gamma$ (°) |
|------------|----------------------------|-------------------------|--------------|
| Case 1     | 70,000                     | 20,000                  | 282          |
| Case 2     | 60,000                     | 60,000                  | 281          |
| Case 3     | 50,000                     | 100,000                 | 280          |
| Case 4     | 40,000                     | 150,000                 | 278          |

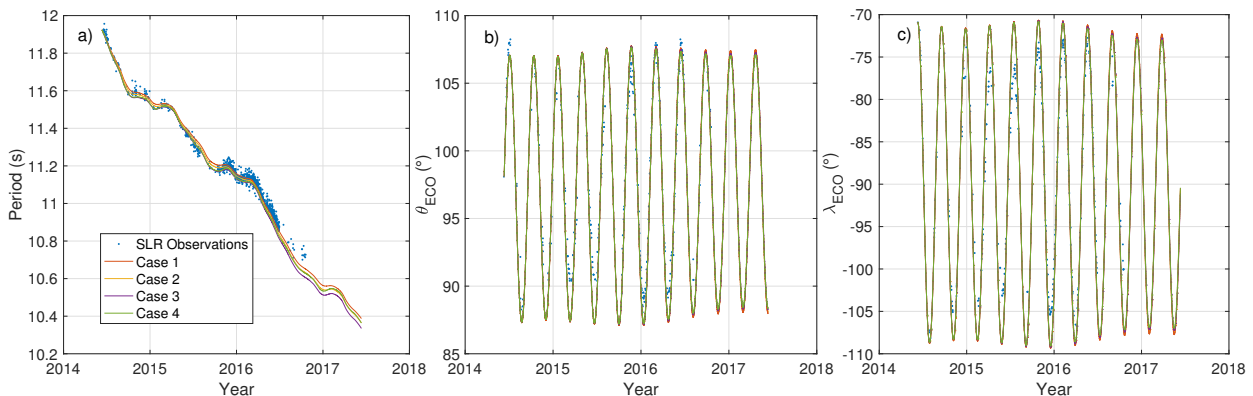


Figure 4: Best Fit Simulations Varying  $I_z$ ,  $M$ , and  $\gamma$  vs. Observations

## 4 Energy Analysis

It is usually expected that energy dissipation eventually transitions a rotating rigid body in space into a major-axis spin; it is in this light that additional simulations were performed with D-SPOSE including the influence of internal energy dissipation, modelled as a Kane damper [5]. The characteristics of the damper were varied: two moments of inertia were considered,  $I_d = 1$  kg m<sup>2</sup> and  $I_d = 10$  kg m<sup>2</sup>; and the damping coefficient  $k_d$  was selected to be 1, 0.1, and 0.01 kg m<sup>2</sup> s<sup>-1</sup>. These damper characteristics led to an initial perturbing torque on the order of  $10^{-7}$  and  $10^{-8}$  N m for the respective damper inertias, compared to approximately  $10^{-2}$ ,  $10^{-4}$ , and  $10^{-5}$  N m for the gravity-gradient, radiation, and eddy-current torques, respectively.

Figure 5 shows the angular velocity and spin axis orientation of TOPEX/Poseidon for the corresponding simulations that were run for a period of three years using the parameters of Case 2

described in Table 1, but with no axisymmetry, randomly choosing  $I_x = 94,800 \text{ kg m}^2$  and  $I_y = 75,000 \text{ kg m}^2$ , in order to have a clear major principal axis.

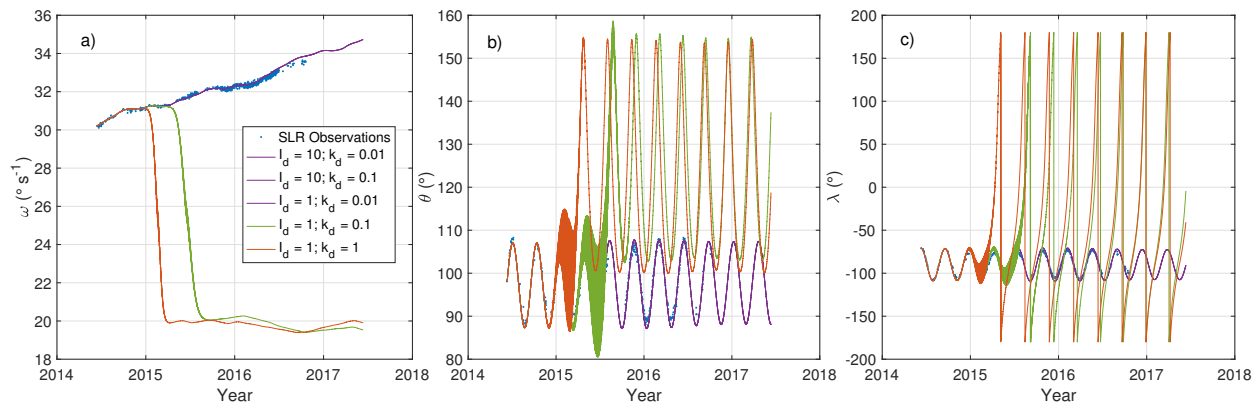


Figure 5: Simulations with Internal Energy Dissipation

As can be seen, for the cases where the effect of internal energy dissipation is expected to be the largest (either due to a small  $I_d$  or a large  $k_d$ ), at some point during the simulation, a transition away from the minor-axis spin and into a major-axis spin occurs. The time taken for the system to transition, however, depends on the damper characteristics, and if internal energy dissipation is small enough, a stable minor-axis spin has the potential to endure for quite some time.

## Acknowledgments

The authors would like to thank Daniel Kucharski for providing the SLR data for TOPEX/Poseidon.

## References

- [1] Sagnieres, L. B. M., “Modeling and Simulation of Long-term Rotational Dynamics of Large Space Debris,” Ph.D. Thesis, McGill University, 2019.
- [2] Holland, R. L., and Sperling, H. J., “A First-Order Theory for the Rotational Motion of a Triaxial Rigid Body Orbiting an Oblate Primary,” *The Astronomical Journal*, 1969, Vol. 74, No. 3, pp. 490-496.
- [3] Kucharski, D., et al., “Photon Pressure Force on Space Debris TOPEX/Poseidon Measured by Satellite Laser Ranging,” *Earth and Space Science*, Vol. 4, 2017, pp. 661-668. doi:10.1002/2017EA000329.
- [4] Cerri, L. and Couhert, A. and Ferrage, P., “DORIS satellites models implemented in POE processing”, International DORIS Service, 2018, SALP-NT-BORD-OP-16137-CN.
- [5] Kane, T. R., and P. M. Barba, “Effects of Energy Dissipation on a Spinning Satellite”, *AIAA J.*, 1966, Vol. 4, pp. 1392-1394.